UKACC International Conference on Control 2012
Cardiff, UK, 3-5 September 2012

Experimental Study of a Capsubot for Two Dimensional Movements

M. Nazmul Huda, Hongnian Yu and Michael J. Goodwin

Abstract— **A capsubot (capsule robot) which works on the principle of internal reaction force has no external moving parts whereas a conventional robot has legs and/or wheels. It is an underactuated mechanical system and has a lot of potential applications such as medical diagnosis, underground pipe leakage detection, rescue work in the hazardous environment etc. However, most capsule robots studied/developed can only move in one dimension (1D). This paper presents the implementation of the recently proposed double parallel mass capsubot which uses two parallel inner masses (IMs) to move the capsubot in two dimensions (2D). A three stage control strategy is proposed to resolve the control issue of underactuated mechanical system. A closed-loop control approach is applied to the IMs of the capsubot. The comparison with the simulation studies are also obtained and analyzed.**

I. INTRODUCTION

Minimally invasive diagnosis and interventions feature safe and reliable techniques and result in shorter hospital stays, less pain, more rapid return to daily work, and improved immunological response compare to the conventional ways. Thus relevant researches have gotten extensive interest to develop minimally invasive devices for surgical and diagnostic applications [1], [2], [3], [4]. Robot-assisted laparoscopic and thoracoscopic surgeries are becoming popular because of its less invasiveness and reliability [5]. Researchers are designing mobile robots to perform abdominal surgery which will further decrease the invasiveness [6], [7], [8].

Passive capsule endoscopy has been used to diagnose GI (gastro-intestinal) tract diseases which is safer for the patient and easier to perform compare to the conventional probe endoscopy. Research is ongoing in order to add mobility to capsule endoscope to increase the reliability, performance and add functionalities such as biopsy, drug delivery, surgery etc. Mobile robots designed for abdominal cavity as well as GI tract can be divided based on the propulsion mechanism used as 1) external propulsion robot (i. magnetic propulsion [9]) 2) internal propulsion robot (i. wheeled [10] ii. legged [11] iii. internal reaction force propulsion robot [12]) and 3) hybrid propulsion robot (combination of external and internal) [13].

The sharp edges of legs or wheels of the internal propulsion robots create the risk to injure the tender GI track and internal organs. Also to perform magnetic propulsion it requires large external magnet [9] which makes the system expensive.

On the contrary the capsubots based on internal reaction force are simple in construction and have no external legs or wheels [14], [15]. The structure of the principle is derived from [16] where impact force and dry friction is utilised to create motion. A mass attached to the main object through a piezoelectric element, is made to move away from the main object rapidly and then to return to the initial position slowly with a sudden stop. The main object moves during the rapid motion and at the stopping moment and remains stationary for the rest of the time. The object can move along a straight line by repeating the above process. In [17] the propulsion principle was analyzed from the viewpoint of physics and a control law and optimum parameters of the system were proposed. In [18], [19], the motion generation of a single mass capsubot was explained on the basis of a four step velocity profile which is, fast motion for first two steps and slow motion in the last two steps. In [15], the motion generation of the capsubot was explained on the basis of a seven step velocity profile which is, fast motion in the first three steps and slow motion in the rest of the steps. A pendulum-driven cart was analysed in [14] with a six step velocity profile. In [12], motion of a single mass capsubot was explained on the basis of a novel four step acceleration profile and a stand-alone prototype was developed based on the profile.

However, except [20] all the capsubots researched so far can only move in one dimension (1D) with their present designs. In practical applications, high dimensional movements of a capsubot is required. In [21] a double-pendulum driven cart was proposed for 2D movements and simulation results was presented. But this cart has wheels and thus lacks the advantages of a capsubot which is legless and wheelless. In [20] a capsubot with 2D movements was proposed and theoretical analysis was performed. In this paper practical implementation of the capsubot proposed in [20] is presented. The experimental results are analyzed and compared with the theoretical results.

The paper is structured as below. Section II presents the modelling and motion generation of the capsubot. Prototyping and programming of the capsubot prototype is explained in section III. Section IV proposes a control strategy for the underactuated mechanical system and explains the control of the 2D capsubot. Section V presents experimental results, compares them with simulation results and analyses them. Finally in section VI the paper is concluded and future direction of the research is presented.

This work has been supported by the European Erasmus-Mundus Sustainable eTourism project 2010-2359, the EPSRC UK-Japan Network on Human Adaptive Mechatronics Project (EP/E025250/1) and EU Erasmus Mundus Project-ELINK (EM ECW-ref.149674-EM-1- 2008-1-UK-ERAMUNDUS). The authors thank Mr. Sam Wane and Dr Ian Moorcroft for their comments and assistances while performing this research.

M. Nazmul Huda, Hongnian Yu and Michael J. Goodwin are with the Faculty of Computing, Engineering and Technology, Staffordshire University, UK. Email: {m.n.huda, h.yu and m.j.goodwin}@staffs.ac.uk

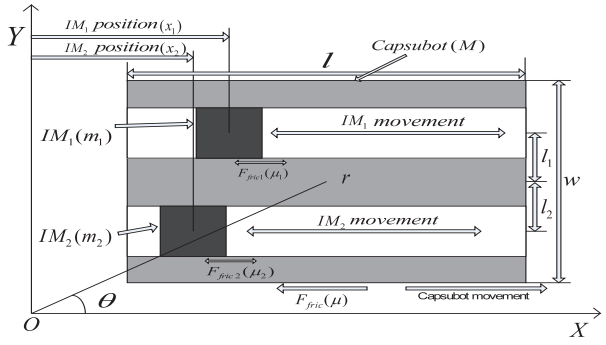

Fig. 1. Schematic diagram of double parallel mass capsubot [20]

II. Modelling and Motion Generation

A. Dynamic Modelling

The capsubot proposed in [20] is shown in Fig. 1. Two IMs are placed in the hollow spaces within the capsubot. IMs can move along the hollow spaces. By controlling the movements of IMs the capsubot can be moved in a 2D plane. It can perform linear, rotational, and 2D motions.

The capsubot dynamic models are as follows [20]:

$$F_i = m_i\ddot{x}_i + sgn(\dot{x}_i - \dot{r})\mu_i m_i g \quad \forall \ i = 1, 2 \tag{1}$$

$$\sum F = -m_1\ddot{x}_1 - m_2\ddot{x}_2 = M\ddot{r} + sgn(\dot{r})\mu M g \tag{2}$$

$$\sum M_G = m_2\ddot{x}_2 l_2 - m_1\ddot{x}_1 l_1 = I\ddot{\theta} + M_f \tag{3}$$

where $sgn(\dot{x}_i - \dot{r})\mu_i m_i g$ is the friction force between the IM_i and the capsubot; $sgn(\dot{r})\mu M g$ is the friction force between the capsubot with the environment; $M_f = sgn(\dot{\theta})\frac{2}{3}\mu_r P(r_2 + \frac{wl - \pi r_2^2}{\pi r_1})$ [20] is the frictional moment of the capsubot with surface of movement and $I = \frac{1}{12}M(l^2 + w^2)$ is the moment of inertia of the capsubot about z-axis through the mass centre of the capsubot. Rest of the parameters are explained in Table I.

B. Motion Generation

In motion generation, we consider the following 3 cases: 1) Linear motion; 2) Rotational motion and 3) 2D motion. Here we design that $m_1 = m_2$ and $l_1 = l_2$.

1) Linear Motion: If both the IMs move with same acceleration i.e $\ddot{x}_1 = \ddot{x}_2$ then $\sum M_G = 0$, and $\sum F \neq 0$. Thus for linear motion both IMs follow the acceleration profile proposed in [12]. As $\sum M_G = 0$, so $\theta = 0$. Thus, $x = r \ \ and \ \ y = 0$ (using $x = r\cos\theta \ \ and \ \ y = r\sin\theta$).

2) Rotational Motion: If both the IMs move with same acceleration in opposite direction i.e. $\ddot{x}_1 = -\ddot{x}_2$ then $\sum M_G \neq 0$, and $\sum F = 0$. Here one of the IMs follows the acceleration profile same as linear motion. The remaining IM follows an acceleration profile that is same in magnitude but opposite in direction. As $\sum F = 0$, so $r = 0$. Thus, $x = y = 0$. As $\sum M_G \neq 0$, so $\theta \neq 0$.

TABLE I

Parameters of the Capsubot

F_i	Force applied on IM_i
$\sum F$	Resultant reaction force acting on the mass centre of capsubot
$\sum M_G$	Resultant moment on the capsubot about z-axis through the mass centre of the capsubot
m_i	Mass of IM_i (cylindrical rod with extra mass)
x_i	Position of IM_i with respect to an external fixed frame
r	Position of the mass centre of the casubot with respect to an external fixed frame
θ	Angular position of the casubot with respect to an external fixed frame
x	$r\cos\theta$
y	$r\sin\theta$
M	Total mass of the capsubot
w	Width of the capsubot
l	Length of the capsubot
h	Height of the capsubot
μ	Dynamic friction coefficient between capsubot and environment (plywood table)
μ_r	Rotational friction coefficient between capsubot and environment (plywood table)
μ_i	Dynamic friction coefficient between IM_i and linear DC motor (LM_i)
g	Acceleration of gravity
k	Total stroke length in one direction
F_{ipmax}	Maximum peak force on IM_i
F_{icmax}	Maximum continuous force on IM_i
$\ddot{x}_{imax}$	Maximum achievable acceleration of IM_i
l_i	Perpendicular distance of the mass centre of the capsubot from the direction of forces F_i
r_1	$\frac{1}{2}\sqrt{l^2 + w^2}$
r_2	$w/2$
P	Mg

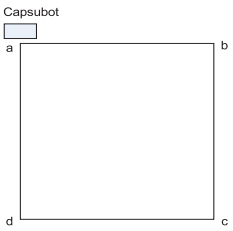

Fig. 2. Squared motion path

3) 2D Motion: By combining the linear and rotational motion, the capsubot can perform a 2D motion. Squared motion, rectangular motion, circular motion etc. are examples of this type of motion.

To travel a-b-c-d-a squared path of Fig. 2 the capsubot would move 'a' to 'b' using linear motion mode and then it would rotate 90 degree using rotational motion mode and then again would use linear motion. By using linear motion and rotational motion alternately the capsubot completes its travel path a-b-c-d-a.

III. Experimental Setup

A prototype shown in Fig. 3(a) has been developed to validate the theoretical analysis performed in [20]. Here the cylindrical rods of two linear DC motors (LM0830-015-01) [22] (see Fig. 4(A)) are used as two IMs. The linear

DC motors (LMs) are placed and attached using adhesive on a housing made of thin paperboard and thus forms the prototype. It is connected to a motion controller through wires. The parameters of the capsubot are listed in Tables I and II.

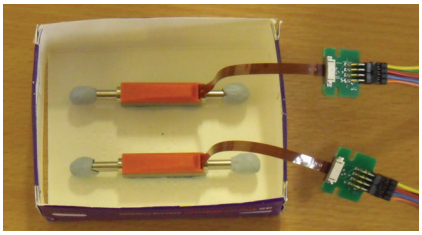

(a) Capsubot prototype

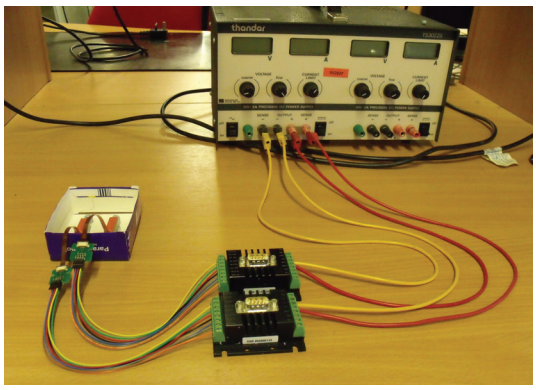

(b) Capsubot prototype with controllers and power supply

Fig. 3. Implemented Capsubot

The main components of the linear DC motor (LM) are a housing or motor shell which houses the coil, Hall sensors, a PCB (printed circuit board) etc. and a cylindrical rod which is a permanent magnet. The cylindrical rod can move back and forth through the housing. The cylindrical rod can move 7.5mm in each direction from its middle position. Here we used 6 mm and left the rest as a clearance. We added extra mass to the both ends of the cylindrical rod to increase the IM mass to capsubot mass ratio. We shall use the term IM (inner mass) for the cylindrical rod with extra mass in the rest of the paper.

The motion of the IM is controlled by the motion controller shown in Fig. 4(B). A linear force is applied to the IM when the coil in the motor shell is energised by the motion controller. The linear DC motor (LM) can be connected to the motion controller through wires and a connector. It takes power from the motion controller. The Hall sensors sense the position of the IM and feed the data to the motion controller to form a closed loop system.

The controller is programmed to move the IM from one location to another location by using a given acceleration and deceleration. The controller by itself calculates the time it has to use for acceleration and then deceleration to reach the desired location. The controller uses three Hall sensors on each linear DC motor (LM) to take feedback about the position of the IM and corrects the input to the IM accordingly to maintain the desired acceleration or deceleration and velocity.

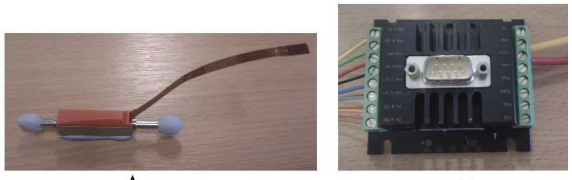

A B

Fig. 4. A) Modified linear DC motor (LM) B) Motion controller

The motion controller is driven by $12V - 30V$ DC which is taken from a DC power supply. The motion controller of the capsubot system is programmed using the Motion Manager software [22] and the program is transferred from PC to the motion controller by a RS-232 cable and stored in the EEPROM of the motion controller. Then the motion controller can be disconnected from the PC. When the motion controller is powered the stored program is executed and the IM moves accordingly. If the motion controller is connected to the PC the Motion Manager software logs the data of the linear DC motor (LM).

IV. CONTROL APPROACH

To use the capsubot in various applications the movement of the capsubot needs to be controlled precisely. The capsubot should be able to change its velocity while moving according to the requirement of the application. Thus we can state the problem as a position or velocity trajectory tracking problem. The capsubot is a underactuated system i.e degrees of freedom to be controlled are greater than number of control inputs. For underactuated systems trajectory tracking is still an open issue to be solved. To solve this problem we divide the problem into three stages which are described below. The schematic diagram of the complete control system is shown in Fig. 5.

- *Stage 1:* For a given trajectory of the capsubot, desired trajectories of IMs are calculated.
- *Stage 2:* For the desired trajectories of the IMs, control inputs i.e forces are calculated (open-loop). The closed-loop control is achieved by correcting the control inputs using the error which is the difference between the measured and the desired trajectories of the IMs.
- *Stage 3:* Feedback should also be taken from the capsubot position and the control input should be corrected according to the error value for tracking the position of the capsubot properly.

In this paper stage 2 of the control system is performed i.e. simulation analysis and experimentation of closed loop control of IMs are performed for the capsubot. Stages 1 and 3 shall be completed in our future research. The schematic diagram of the control system for stage 2 is shown in Fig. 6. By implementing this stage the capsubot can perform linear and rotational motion and by combining these two can perform 2D motion. If the IMs follow a fixed set of accelerations the capsubot would have a constant average

linear or rotational velocity in every cycle. To change the velocity a different set of acceleration has to be chosen.

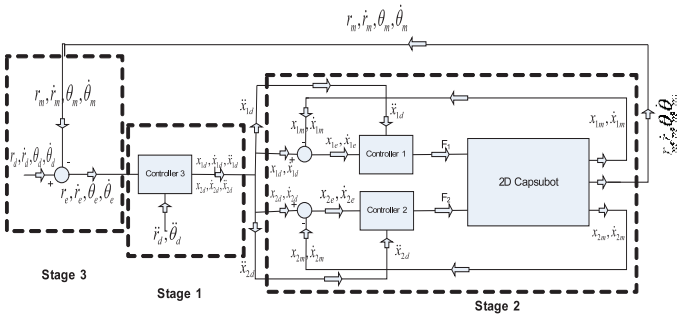

Fig. 5. Schematic diagram of 3-stage control system for capsubot

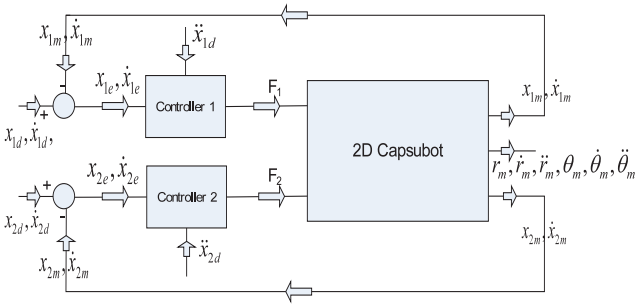

Fig. 6. Schematic diagram of Stage 2 of the control system

Two open loop control laws for the IMs for all the motion cases are:

$$F_{id} = m_i\ddot{x}_{id} + sgn(\dot{x}_{id} - \dot{r}_d)\mu_i m_i g \tag{4}$$

The closed loop control laws for the IMs can be selected, using partial feedback linearization, as [14]:

$$F_{id} = \alpha\tau_{id} + \beta \tag{5}$$

where $\alpha = m_i$ and $\beta = sgn(\dot{x}_{id} - \dot{r}_d)\mu_i mg$

Let $\tilde{x}_i = x_i - x_{id}$ be the tracking error; choosing the linear control law $\tau_{id} = \ddot{x}_i - k_1\dot{\tilde{x}}_i - k_2\tilde{x}_i$ and applying the control laws of (5) to (1) we get,

$$\ddot{\tilde{x}}_i + k_1\dot{\tilde{x}}_i + k_2\tilde{x}_i = 0 \tag{6}$$

The values of k_1 and k_2 can properly be selected using (6). Then by using the control laws of (5) the IMs can be made to follow the desired accelerations, velocities and positions which are given below. The impact of $\dot{r}_d$ on β is neglected in simulation.

From the acceleration profiles in [12] and [20] desired IMs accelerations for linear and rotational motions are given below:

$$\ddot{x}_{id} = \begin{cases} b_{1\_i} & t \in [0, t_1) \\ b_{2\_i} & t \in [t_1, t_3) \\ b_{1\_i} & t \in [t_3, t_4] \end{cases}$$

where b_{1_i} is the acceleration of IM_i in steps 1 and 4; b_{2_i} is the acceleration of IM_i in steps 2 and 3; t_1, t_2, t_3 and t_4 are the time after steps 1, 2, 3 and 4 respectively.

Desired IMs velocities and positions can be calculated from the desired accelerations. All the simulations in this paper are performed using Matlab and Simulink with the help of the control law of (5) and motion equations (1), (2) and (3).

V. EXPERIMENTAL RESULTS AND ANALYSIS

The acceleration of IM_i is constrained by $\ddot{x}_i \leq min(\ddot{x}_{imax}, \frac{F_{icmax}}{m_i})$. Here $\ddot{x}_{imax}$ is $30ms^{-2}$ which is a physical constraint of IM_i. F_{icmax} is the maximum force that can be achieved on the IM_i continuously. On the other hand F_{ipmax} is the maximum force that the IM_i can sustain for a short time. In this experiment maximum acceleration used is $20ms^{-2}$.

The data of IM_s are obtained from the Motion Manager software and then the curves are plotted using Matlab. To obtain the data for capsubot movements we recorded the motion of the capsubot using a video camera and then a video analysis software Quintic Biomechanics [23] was used to calculate the position, velocity and acceleration.

A. Experimental Results

- Linear Motion: Fig. 7(a) shows the positions of IM_1 and IM_2, and Fig. 7(b) shows the currents of LM_1 and LM_2 for linear motion. We can see that the IMs move in the range of -6 mm to 6 mm with a cycle period of 0.15s. The shape of the curves of positions are similar with a very small difference. Motor currents are also similar in patterns though there is a small difference between them.
- Rotational motion: Fig. 8(a) shows the positions of IM_1 and IM_2, and Fig. 8(b) shows the currents of LM_1 and LM_2 for rotational motion. We can see that the two IMs move in the range of -6 mm to 6 mm in the opposite direction with a cycle period of 0.15s. Though the IMs are moving in the opposite direction the motor currents are similar in patterns as the magnitude of the accelerations are same.

B. Comparison with Simulation

The parameters for the simulation of the capsubot is taken from the developed prototype and are listed in Table II.

Figs. 9(a)-9(d) and 10(a)-10(d) show the comparison between experimental and simulation results for the linear motion and rotational motion. For the linear motion both IMs has the same acceleration profile. Thus comparison for IM_1 is shown only in Figs. 9(a)-9(d). For the rotational motion one of the IMs follows the same acceleration profile as the linear motion and the other IM follows an acceleration profile that is opposite to the previous one. Thus for the rotational motion comparison for IM that has the opposite acceleration profile i.e. IM_2 is shown in Figs. 10(a)-10(d).

Although there are some differences between the experimental and simulation results, their trends are similar.

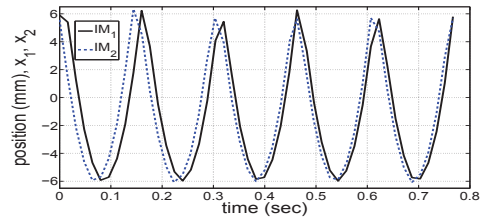

(a) IM_1 and IM_2 positions for linear motion

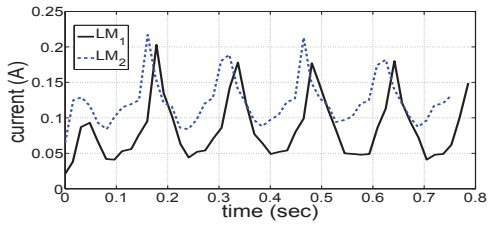

(b) Currents of LM_1 and LM_2 for linear motion

Fig. 7. Experimental results for linear motion

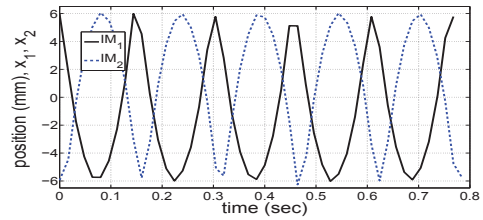

(a) IM_1 and IM_2 positions for rotational motion

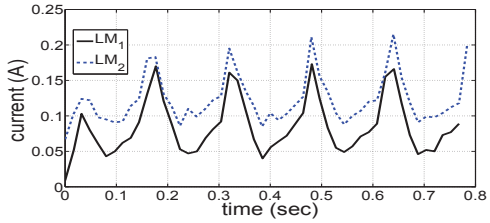

(b) Currents of LM_1 and LM_2 for rotational motion

Fig. 8. Experimental results for rotational motion

The differences may be due to several reasons, such as motor dynamics, sensor dynamics, the other disturbances etc. which are not considered in the simulation model. We will investigate these issues further in future experiments.

From Figs. 9(d) and 10(d) we see that in the linear motion mode the capsubot moves with 8.4 mm/s average velocity. To move the capsubot in the opposite direction we just need to change the acceleration of the IMs to the opposite direction. In the rotational motion the capsubot moves with 13 degrees/s average angular velocity. To rotate the capsubot in the opposite direction we need to swap the acceleration profiles between the IMs.

By using the linear motion and rotational motion alternately the capsubot can move in a 2D plane.

TABLE II

PARAMETER VALUES OF THE CAPSUBOT

m_1, m_2	μ_1, μ_2	k	w	l	h
$6.4gm$	0.2	$6mm$	$7cm$	$8.7cm$	$3.2cm$
g	M	F_{max}	l_1,l_2	μ_r	μ
$9.8ms^{-2}$	$42.9gm$	$1.03N$	$11.5mm$	0.08	0.28
F_{ipmax}	F_{icmax}		Linear	b_{1_1}, b_{1_2}	b_{2_1}, b_{2_2}
$2.74N$	$1.03N$		Motion	$-20m/s^2$	$5m/s^2$
Rotational	b_{1_1}	b_{1_2}	b_{2_1}	b_{2_2}	
Motion	$-20m/s^2$	$20m/s^2$	$5m/s^2$	$-5m/s^2$	

VI. CONCLUSIONS AND FUTURE WORKS

This paper has investigated the 2D capsubot from both simulation and experimentation. The paper has the following contributions: 1) proposed a control strategy for the motion control of underactuated mechanical systems which is an open problem till date; 2) validated the early proposed 2D capsubot design [20] through an initial experimentation; 3) implemented the closed-loop control strategy for the IMs of the 2D capsubot; 4) conducted both simulation and experimentation; 5) compared the experimental and simulation results for demonstrating the proposed capsule robot movability; 6) proposed measuring the position/velocity of a capsubot using video analysis software.

This has built our confidence to conduct further research along this line. We will conduct further experimental test using different control approaches. Also we will select/propose more realistic friction model and validate its performance in different environments.

REFERENCES

[1] P. Dario, B. Hannaford, and A. Menciassi, "Smart surgical tools and augmenting devices," *IEEE Transactions on Robotics and Automation*, vol. 19, no. 5, pp. 782–792, 2003.

[2] N. Patronik, T. Ota, M. Zenati, and C. Riviere, "A miniature mobile robot for navigation and positioning on the beating heart," *IEEE Transactions on Robotics*, vol. 25, no. 5, pp. 1109–1124, 2009.

[3] C. Briggs, C. Mann, G. Irving, C. Neal, M. Peterson, I. Cameron, and D. Berry, "Systematic review of minimally invasive pancreatic resection," *Journal of Gastrointestinal Surgery*, vol. 13, no. 6, pp. 1129–1137, 2009.

[4] P. Gomes, "Surgical robotics: Reviewing the past, analysing the present, imagining the future," *Robotics and Computer-Integrated Manufacturing*, vol. 27, no. 2, pp. 261–266, 2011.

[5] C. Braumann, C. Jacobi, C. Menenakos, M. Ismail, J. Rueckert, and J. Mueller, "Robotic-assisted laparoscopic and thoracoscopic surgery with the da vinci system: a 4-year experience in a single institution," *Surgical Laparoscopy Endoscopy & Percutaneous Techniques*, vol. 18, no. 3, p. 260, 2008.

[6] A. Lehman, K. Berg, J. Dumpert, N. Wood, A. Visty, M. Rentschler, S. Platt, S. Farritor, and D. Oleynikov, "Surgery with cooperative robots," *Computer Aided Surgery*, vol. 13, no. 2, pp. 95–105, 2008.

[7] A. Lehman, M. Rentschler, S. Farritor, and D. Oleynikov, "The current state of miniature in vivo laparoscopic robotics," *Journal of Robotic Surgery*, vol. 1, no. 1, pp. 45–49, 2007.

[8] S. Ohno, C. Hiroki, and W. Yu, "Design and manipulation of a suction-based micro robot for moving in the abdominal cavity," *Advanced Robotics*, vol. 24, no. 12, pp. 1741–1761, 2010.

[9] M. Nokata, S. Kitamura, T. Nakagi, T. Inubushi, and S. Morikawa, "Capsule type medical robot with magnetic drive in abdominal cavity," in *2nd IEEE RAS & EMBS International Conference on Biomedical Robotics and Biomechatronics*, pp. 348–353, 2008.

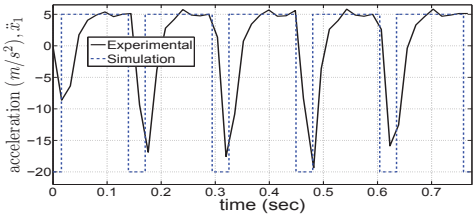

(a) Acceleration of IM_1 for linear motion

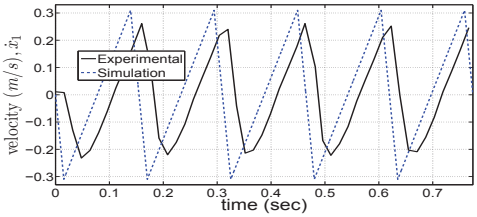

(b) Velocity of IM_1 for linear motion

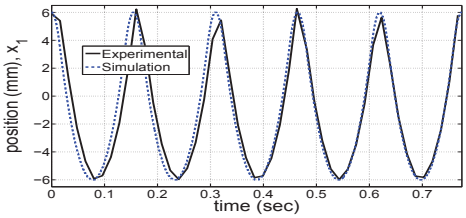

(c) Position of IM_1 for linear motion

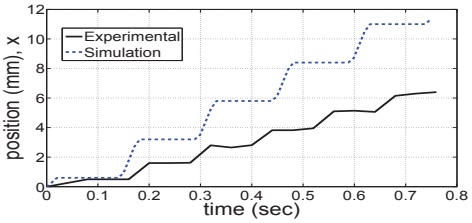

(d) Position of the capsubot for linear motion

Fig. 9. Comparison between experimental and simulation results for linear motion

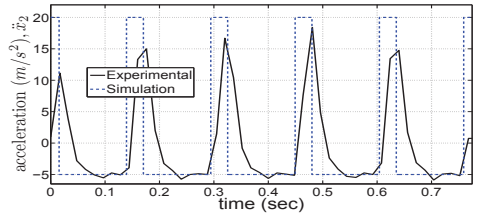

(a) Acceleration of IM_2 for rotational motion

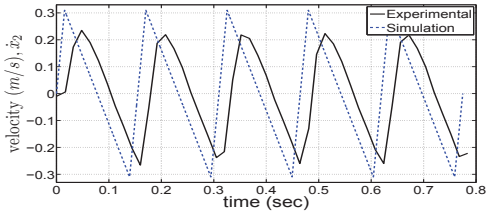

(b) Velocity of IM_2 for rotational motion

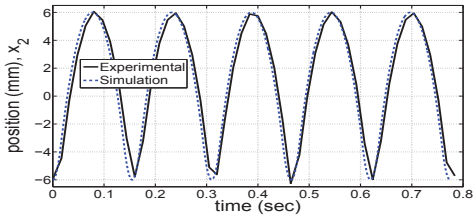

(c) Position of IM_2 for rotational motion

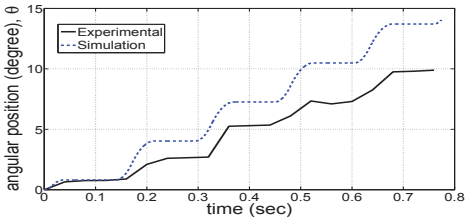

(d) Angular position of the capsubot for rotational motion

Fig. 10. Comparison between experimental and simulation results for rotational motion

[10] S. Platt, J. Hawks, and M. Rentschler, "Vision and task assistance using modular wireless in vivo surgical robots," *IEEE Transactions on Biomedical Engineering*, vol. 56, no. 6, pp. 1700–1710, 2009.

[11] P. Valdastri, R. Webster, C. Quaglia, M. Quirini, A. Menciassi, and P. Dario, "A new mechanism for mesoscale legged locomotion in compliant tubular environments," *IEEE Transactions on Robotics*, vol. 25, no. 5, pp. 1047–1057, 2009.

[12] H. Yu, M. N. Huda, and W. S. O., "A novel acceleration profile for the motion control of capsubots," in *IEEE International Conference on Robotics and Automation*, pp. 2437–2442, 2011.

[13] M. Simi, P. Valdastri, C. Quaglia, A. Menciassi, and P. Dario, "Design, fabrication, and testing of a capsule with hybrid locomotion for gastrointestinal tract exploration," *Mechatronics, IEEE/ASME Transactions on*, vol. 15, no. 2, pp. 170–180, 2010.

[14] H. Yu, Y. Liu, and T. Yang, "Closed-loop tracking control of a pendulum-driven cart-pole underactuated system," *Proceedings of the Institution of Mechanical Engineers, Part I: Journal of Systems and Control Engineering*, vol. 222, no. 2, pp. 109–125, 2008.

[15] Y. Liu, H. Yu, and T. Yang, "Analysis and Control of a Capsubot," in *Proceedings of the 17th World Congress the International Federation of Automatic Control*, July 2008.

[16] Y. Yamagata and T. Higuchi, "A micropositioning device for precision automatic assembly using impact force of piezoelectric elements," in *1995 IEEE International Conference on Robotics and Automation*, vol. 1, pp. 666–671, May 1995.

[17] F. Chernous'ko, "The optimum rectilinear motion of a two-mass system," *Journal of applied Mathematics and Mechanics*, vol. 66, no. 1, pp. 1–7, 2002.

[18] N. Lee, N. Kamamichi, H. Li, and K. Furuta, "Control system design and experimental verification of capsubot," in *IEEE/RSJ International Conference on Intelligent Robots and Systems*, pp. 1927–1932, 2008.

[19] G. Su, C. Zhang, R. Tan, and H. Li, "A linear driving mechanism applied to capsule robots," in *International Conference on Networking, Sensing and Control, 2009. ICNSC'09*, pp. 206–209, 2009.

[20] M. N. Huda and H. Yu, "Modelling and motion control of a novel double parallel mass capsubot," in *18th World Congress of the International Federation of Automatic Control (IFAC)*, pp. 8120–8125, 2011.

[21] Y. Liu, H. Yu, and S. Cang, "Modelling and motion control of a double-pendulum driven cart," *Proceedings of the Institution of Mechanical Engineers, Part I: Journal of Systems and Control Engineering*, vol. 226, no. 2, pp. 175–187, 2012.

[22] S. MINIMOTOR SA, "http://www.faulhaber-group.com/." Online.

[23] Q. Biomechanics, "http://www.quintic.com/." Online.